Reconstructing the Climate Variability During the Last 5000 Years From the Banni Plains, Kachchh, Western India

Nisarg Makwana[1], S. P. Prizomwala[1], Archana Das[1]*, Binita Phartiyal[2], Aashima Sodhi[1,3] and Chintan Vedpathak[1,3]

[1]Institute of Seismological Research, Gandhinagar, India, [2]Birbal Sahni Institute of Paleosciences, Lucknow, India, [3]Research Scholar, Gujarat University, Ahmedabad, India

The climatic conditions during the beginning of the last 5,000 years have been discussed, debated, and documented from various parts of the Indian subcontinent, due to the human–climate interrelationship. In the present study, we report a multi-proxy dataset encompassing the widely used ∼ geochemical and mineral magnetic proxies supported by radiocarbon and optical chronologies from the Banni Plains of the Rann of Kachchh, western India. Our results support the earlier observations of the prolonged wetter climatic condition synchronous with the mature phase of Harappan era which witnessed a short and intense arid condition at the terminal part of the mature Harappan phase. The climate system dramatically fluctuated during the last five millennia from pulsating between relatively arid (4,800–4,400 years BP, 3,300–3,000 years BP, and at 2,400 years BP) and relatively humid phases (>4,800 years BP, 4,000–3,300 years BP, 1900–1,400 years BP, and 900–550 years BP). The multi-proxy dataset shows a gradual strengthening of the monsoonal conditions from the Banni Plains during the late Harappan phase. Apart from this, the high sedimentation rate (>1 mm/yr) recorded from the Banni Plains suggests it can be tapped as a robust archive to reconstruct multi-decadal to centennial climatic events spanning the Holocene epoch.

Keywords: paleoclimate, Banni plains, middle to late Holocene, Kachchh, Harappan civilization 2

INTRODUCTION

Southwest Indian monsoon has a high socioeconomic impact as it plays a key role in delivering annual rainfall (nearly 80%) in the Indian subcontinent (Anderson et al., 2010; Berkelhammer et al., 2010). An understanding of the variability of Indian summer monsoon (ISM) rainfall for the Holocene epoch is vitally required to assess the speculated link between the climate deterioration and the decline in ancient civilization. The mid-Holocene, in particular, has witnessed several changes in climate with abrupt short events recorded globally as well as in the Indian subcontinent (Lamb, 1985; Bianchi and Mc Cave, 1999; Anderson et al., 2010; Sanwal et al., 2013; Quamar and Chauhan, 2014; Ngangom et al., 2016). Prasad et al. (2007), Prasad et al. (2014 b) reported wetter climate during the 5.5 to 2.8 ka BP from the lacustrine environments of Mainland Gujarat. Similarly, Laskar et al. (2013) reported subhumid climatic conditions from fluvial sediments of the Mainland Gujarat region. The period between 2.8 and 1.3 ka has reportedly experienced arid conditions from the lacustrine and fluvial records of Mainland Gujarat (Laskar et al., 2013a; Prasad V. et al., 2014; Sridhar et al., 2014a). Raja et al. (2019) reported paleoflood activity during 4,773 cal yr BP from the Parsons Valley Lake, Tamil Nadu. Consequently, the mid-to-late Holocene tend to have recorded various centennial

scaled abrupt climatic variations. However, studies documenting the climatic variations on the centennial to decadal scale are still limited and need to be looked upon (Binanchi and Mc Cave, 1999; Gupta et al., 2003; Sinha et al., 2007; Chauhan et al., 2009; Makwana et al., 2019).

The Great Rann of Kachchh (GRK) in western India is a semi-enclosed basin and a dominantly depositional microenvironment, and hence the paleo-mudflats of Rann have proven to be useful to decipher past climatic oscillation in different timescales (Pillai et al., 2017, 2018; Basu et al., 2019; Makwana et al., 2019). The recent efforts have hinted that the Rann sediments remain a treasure trove for reconstructing Holocene paleoclimate (Ngangom et al., 2016; Pillai et al., 2017, 2018; Basu et al., 2019; Makwana et al., 2019; Sengupta et al., 2019; Sarkar et al., 2020). The Rann of Kachchh is believed to be a Holocene sediment depocenter (Maurya et al., 2013) and also has been a hotspot of mature and late Harappan occupation, which believed to be a riverine and trade-oriented civilization during 7000 BP to 3900 BP (Gaur et al., 2013; Sarkar et al., 2020). Large urban centers of mature Harappan settlements flourished along the Indus and Ghaggar-Hakra rivers (Possehl, 2002), and were considered to have abruptly ended around 3,900 years BP (Possehl, 2002). Also, the mid-Holocene climatic changes are coincident with the appearance of highly organized and urbanized civilizations from the Afro-Asiatic monsoonal region such as Egypt, Mesopotamia, Indus-Saraswati, and in northern China regions that form the bulk of the deserts today (Brooks, 2006; Prasad V. et al., 2014). However, the reasons for the decline of these civilizations, viz. abrupt climate change, sea level fluctuation, or reduction of natural resources, are still a question of debate for the researchers (Galili 1988; Staubwasser et al., 2003; Wright et al., 2008; Giosan et al., 2012; Dixit et al., 2014, 2018; Das et al., 2017; Sengupta et al., 2019).

Some of the intriguing questions regarding the paleoclimatic conditions, particularly, in the Kachchh region of western India are as follows: 1) What were the paleoenvironmental conditions that existed in the Banni Grassland during the middle-to-late Holocene? 2) How did the climatic fluctuations change since the mature Harappan times? In light of this, the objective of the present study is to reconstruct the past climatic events from the Banni Plains and explore their nature/boundary conditions during the last 5,000 years using a multi-proxy dataset.

STUDY AREA

The GRK is a unique and intriguing vast salt encrusted flat land, which is an E–W trending subbasin and occupies almost half of the area of the seismically active Kachchh paleo-rift basin (Burnes, 1834; Glennie and Evans, 1976; Biswas, 1987). The Banni Plain is a part of the extensive low-level hyper arid saline tract of the Great Rann that occupies the northern part of the seismically active Kachchh paleo-rift basin. The Banni grassland happens to be only the inhabited part of the Great Rann due to the fact that it occurs at the highest elevation and is free of present-day marine submergence (Roy and Merh, 1981). Large

parts of the Banni get submerged during monsoon under a thin sheet of water by rainfall and rivers from the Kachchh mainland in the south.

The present study site BKR (23°32′48.12″N and 69°40′30.36″E) is situated in the central to the northern part of the Banni Plains (**Figure 1**). The Banni Plains and the GRK are covered by the quaternary deposits mostly comprising silt and clay sediments and considered as Holocene depocenters (Gupta, 1975; Maurya et al., 2013; Khonde et al., 2017a; Makwana et al., 2019) of three distinct sources, viz. Indus source from north, Aravalli in east, and Kachchh Mainland in south (Maurya et al., 2013; Khonde et al., 2017a, b). It experiences a hyper-arid to arid climate with annual rainfall less than 30 mm per year (**Figure 1**). However, till now there are limited data pertaining to the paleoclimate, provenance, and the nature of sediment comprising the Banni Plain. With an aim to study the evolution of these majestic landscape features, which probably beholds vital insights on middle-to-late Holocene climatic fluctuations, a shallow trench from the paleo-mudflat of the Banni Grassland has been investigated. Trench is 5.5 m deep (BKR site) and located on Bhuj-Khavda road (**Figure 1**) in the Banni Plains. Geomorphologically, the study site is surrounded by higher Banni surface with an elevation varying from 4 to 12 m amsl. The elevation of the trench site was 4.4 m above the present day mean sea level (msl) measured based on a D-GPS survey. The studied site is away from any human settlement, which assures negligible to nil anthropological effect.

ANALYTICAL METHODS

Sediment Geochemistry

Al_2O_3, Fe_2O_3, and TiO_2 are the major components of the aluminosilicate phase group and are useful to deduce the post depositional weathering and paleoenvironmental condition that prevailed in the region (Nesbitt and Young, 1982; Agnihotri et al., 2003; Tyagi et al., 2012; Das et al., 2017). Similarly, the ratio of K_2O/Al_2O_3 and CIA (Chemical Index of Alteration) has been used to measure the chemical weathering intensity in the region (Nesbitt and Young, 1982; Buggle et al., 2011; Pillai et al., 2018). The natural samples in the near-shore and marine-influenced environments may contain CaO content, originating from marine organisms. Hence, the samples collected from the field were treated with 1 N HCl until the CaO fraction was removed. These decarbonated samples were then used for estimating CIA, which represents the detrital content, originating due to the chemical weathering in the source region. A total of 55 samples were collected from the BKR site and dried at 50°C, crushed, homogenized, and sieved to <63 µm size. A part of this fraction was used for the analysis in XEPOS HE XRF instrument at the Institute of Seismological Research, India. The analytical precision of major oxide was better than 5% and that of trace elements was better than 10% (Das et al., 2017; Makwana et al., 2019).

Mineral Magnetic Measurements

Environmental magnetic properties of sediment samples were measured using standard rock magnetic methods (Walden et al.,
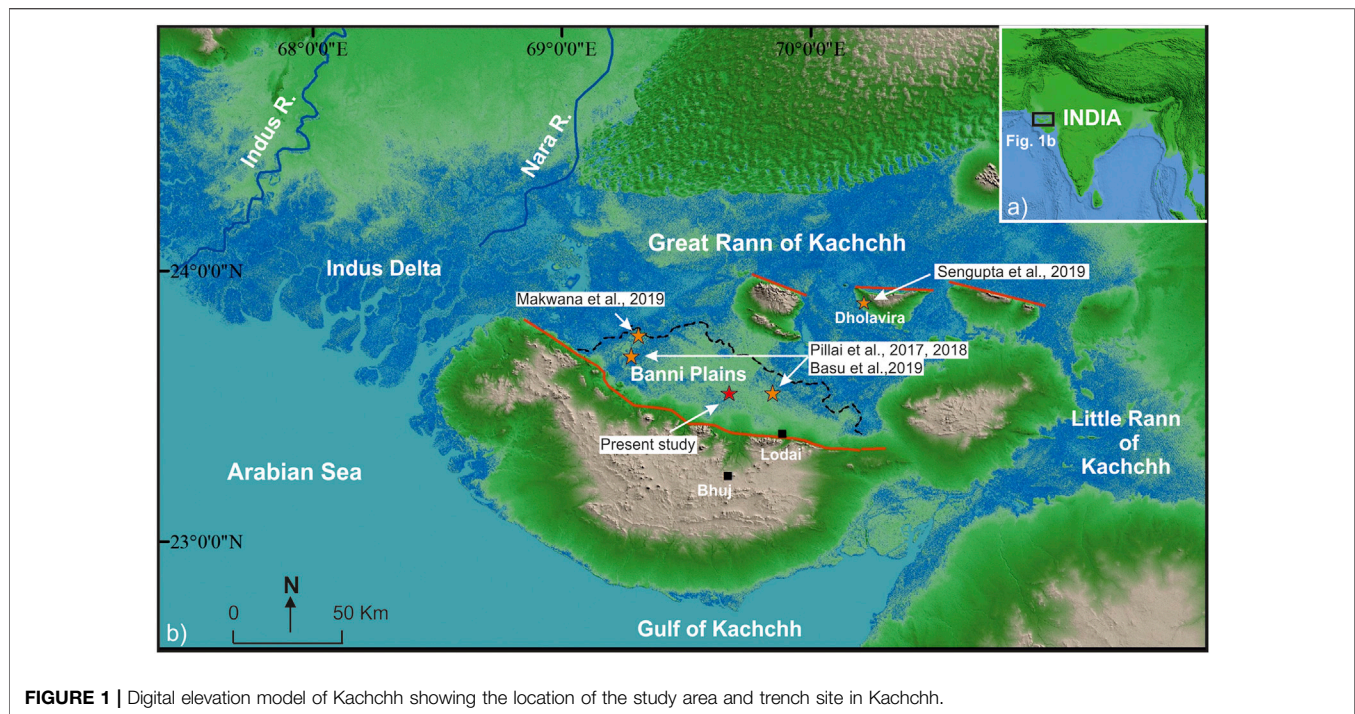
FIGURE 1 | Digital elevation model of Kachchh showing the location of the study area and trench site in Kachchh.

1999; Warrier and Shankar, 2009; Basavaiah, 2011). Selected samples were oven-dried and packed, ensuring no movement of magnetic minerals in nonmagnetic plastic bottles of 10 cm^3 for analysis. In the present study, we have measured magnetic susceptibility (χ), anhysteretic remnant magnetization (ARM), and isothermal remnant magnetization (IRM) at Birbal Sahni Institute of Palaeosciences, Lucknow, India. Low magnetic susceptibility (χ_{LF}) was measured using a Bartigton MS2B dual-frequency susceptibility meter at 976 Hz frequency. Samples were first demagnetized by using the AF demagnetizer, and then anhysteretic remnant magnetization (ARM) was calculated in a steady 0.05_{mT} field superimposed over decreasing alternating field (AF) up to 100_{mT} using the alternating field demagnetizer, D-2000 AF demagnetizer. The remnant magnetization of all ARMs and IRMs was measured using a AGICO JR-6 dual speed spinner magnetometer. Isothermal remnant magnetization (IRM) was measured at forward fields of 20 and 1000_{mT} and backward fields of -20, -40, -60, -100, and -300_{mT} using ASC scientific impulse magnetizer. IRM measured at 1_T field was considered as saturation isothermal remnant magnetization (SIRM). The S-ratio is indicative of the ferrimagnetic vs. anti-ferrimagnetic minerals, and the value close to one corresponds to the dominance of the ferrimagnetic minerals. S-ratio is often used as paleo-monsoonal proxy calculated using the formula IRM$_{-0.3T}$/SIRM (Basavaiah and Khadkikar, 2004).

AMS C-14 Dating

AMS is a modern and more efficient radiocarbon dating method for younger time frames to measure long-lived radionuclide that occurs naturally in environment. We have used two different samples of handpicked foraminifera from unit 2 to estimate the

TABLE 1 | Lithostratigraphic information for the BKR trench site, Kachchh.

Litho-units	Thickness (in cm)	Textural class
Unit-3	170	Clayey silt horizon with faint laminations
Unit-2	330	Silty clay horizon
Unit-1	70	Sticky dark bluish clay horizon

age of sediment deposition. Foraminifera tests were separated out from the samples and sent to Poznan Radiocarbon Laboratory, Poland, for AMS ^{14}C dating. For both the uncalibrated ages, we used a marine reservoir effect (ΔR) of -8 ± 37 from northern Arabian Sea, as it was the closest possible value available from the studied point and represented similar semi-enclosed environment (Dutta et al., 2001). We used the latest available online CALIB 8.2 program for Marine13 dataset (Stuiver et al., 2018). Calibrated ages are expressed as calendar years over a 2σ-error range (95.4%).

RESULTS

Stratigraphy and Chronology of the BKR Trench

Based on the visual observations of sedimentological, textural, structures and variation in color, the entire succession was divided into three major litho-units (**Table 1**). At the BKR trench site, the bottommost exposed unit is a 70-cm-thick sticky dark bluish clay horizon (unit-1), followed by a 330-cm-thick brown silty clay deposit (unit-2). The foraminifera tests were collected from this unit, which yielded a calibrated AMS ^{14}C age of 3,157–3,520 cal yr BP (median value: 3,339 ± 181 cal yr BP)

Sample ID	Depth of sample (m)	Conventional C[14] radiocarbon age (yr BP)	Calibrated age (cal yr BP, ± 2σ)	Median age (cal yr BP, ± 2σ)
POZ-101421	2.3	3,600 ± 35	3,157–3,520	3,339 ± 181
POZ-112296	4.1	4,460 ± 220	3,833–5,032	4,432 ± 600
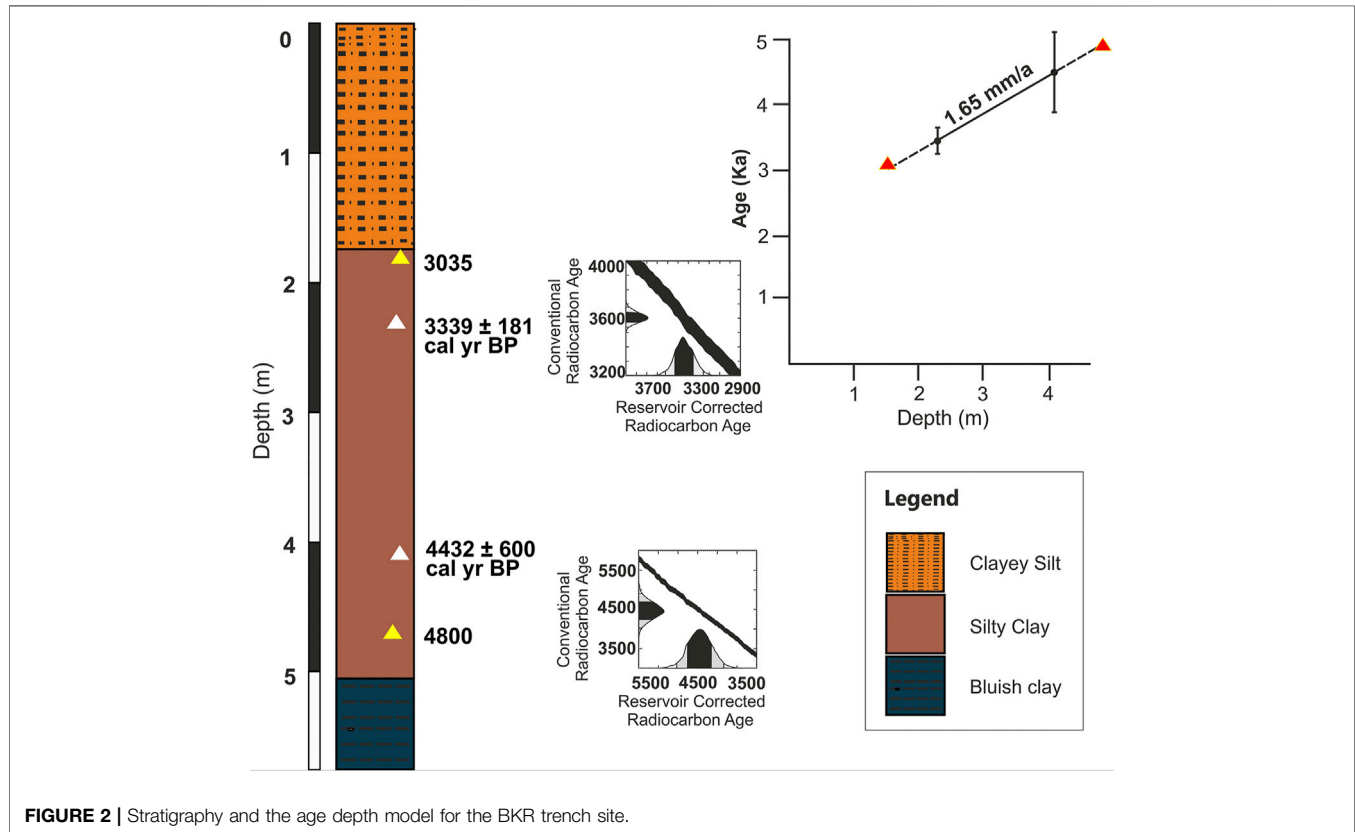
FIGURE 2 | Stratigraphy and the age depth model for the BKR trench site.

and 3,833–5,032 cal yr BP (median value: 4,432 ± 600 cal yr BP) (**Table 2**) at depth of 2.3 and 4.1 m, respectively, from the top of the trench surface. Unit-2 is overlain by 170-cm-thick clayey silt dominated horizon with faint laminations, that is, Unit-3 (**Figure 2**). Owing to the lack of datable material and negligible amount of foraminifers, the bottom age of 4,432 ± 600 cal yr BP shows a wider error scatter, due to mixing of foraminifer tests from two adjacent samples. Hence, due to the lack of available chronology, we assumed a relatively uniform sedimentary sequence in Unit-2 to extrapolate two ages, that is, 4,800 years BP and 3,035 years BP on the basis of the sedimentation rate between the dated depths.

Major Oxide Concentration and Their Elemental Ratio Variation

The concentration of major oxides and trace elements along with their ratios were studied and based on significant deviations in statistical parameters; a total of three relatively arid and four

humid phases of paleoclimatic conditions are deduced (**Supplementary Table 1**).

Zone 1

Zone 1 encompassing the concentration variation of Al_2O_3, Fe_2O_3, and TiO_2 from 14.33 to 15.62%, 4.75 to 5.48%, and 0.73 to 0.80%, respectively. The oxide ratios of K_2O/Al_2O_3, Na_2O/TiO_2, CaO/TiO_2, and Fe_2O_3/TiO_2 varied from 0.17 to 0.19, 1.58 to 2.56, 11.34 to 12.52, and 6.50 to 6.91, respectively. Similarly, the elemental concentration of Sr and Ca varied from 202 to 211 ppm and 6.3 to 6.7%, respectively. The ratios of Zr/Al varied from 15.1 to 21.0. The values of weathering intensity CIA varied from 82 to 85 (**Supplementary Table 1**).

Zone 2

Zone 2 shows the concentration of Al_2O_3, Fe_2O_3, and TiO_2 varied from 13.9 to 15.2%, 4.2 to 5.4%, and 0.76 to 0.81%, respectively. The oxide ratios of K_2O/Al_2O_3, Na_2O/TiO_2, CaO/TiO_2, and Fe_2O_3/TiO_2 varied from 0.17 to 0.19, 1.6 to 2.1, 11.3 to 12.8,

and 5.6 to 6.7, respectively. Similarly, the elemental concentration of Sr and Ca varied from 207 to 223 ppm and 6.4 to 6.9%, respectively. The ratios of Zr/Al varied from 19.0 to 26.5. The values of weathering intensity CIA varied from 79 to 83 (**Supplementary Table 1**).

Zone 3

Zone 3 suggests the concentration of Al_2O_3, Fe_2O_3, and TiO_2 varied from 16.0 to 16.7%, 5.3 to 6.9%, and 0.78 to 0.86%, respectively. The oxide ratios of K_2O/Al_2O_3, Na_2O/TiO_2, CaO/TiO_2, and Fe_2O_3/TiO_2 varied from 0.18 to 0.21, 1.3 to 1.6, 9.3 to 11.4, and 6.6 to 8.0, respectively. Similarly, the elemental concentration of Sr and Ca varied from 179 to 205 ppm and 5.7 to 6.5%, respectively. The ratios of Zr/Al varied from 10.0 to 15.4. The values of weathering intensity CIA varied from 84 to 88 (**Supplementary Table 1**).

Zone 4

Zone 4 suggests the concentration of Al_2O_3, Fe_2O_3, and TiO_2 varied from 14.3 to 15.3%, 4.1 to 5.1%, and 0.71 to 0.76%, respectively. The oxide ratios of K_2O/Al_2O_3, Na_2O/TiO_2, CaO/TiO_2, and Fe_2O_3/TiO_2 varied from 0.16 to 0.18, 1.7 to 2.1, 12.0 to 13.4, and 5.8 to 6.7, respectively. Similarly, the elemental concentration of Sr and Ca varied from 204 to 218 ppm and 6.5 to 6.8%, respectively. The ratios of Zr/Al varied from 16.5 to 20.2. The values of weathering intensity CIA varied from 82 to 85 (**Supplementary Table 1**).

Zone 5

Zone 5 suggests the concentration of Al_2O_3, Fe_2O_3, and TiO_2 varied from 13.7 to 16.4%, 3.9 to 5.1%, and 0.65 to 0.77%, respectively. The oxide ratios of K_2O/Al_2O_3, Na_2O/TiO_2, CaO/TiO_2, and Fe_2O_3/TiO_2 varied from 0.16 to 0.17, 1.72 to 1.88, 11.8 to 15.8, and 5.7 to 6.7, respectively. Similarly, the elemental concentration of Sr and Ca varied from 199 to 220 ppm and 6.3 to 7.3%, respectively. The ratios of Zr/Al varied from 14.8 to 21.2. The values of weathering intensity CIA varied from 82 to 86 (**Supplementary Table 1**).

Zone 6

Zone 6 suggests the concentration variation of Al_2O_3, Fe_2O_3, and TiO_2 between 13.2–13.5%, 3.4–3.8%, and 0.61–0.73%, respectively. The oxide ratios of K_2O/Al_2O_3, Na_2O/TiO_2, CaO/TiO_2, and Fe_2O_3/TiO_2 varied from 0.16 to 0.17, 1.5 to 1.9, 14.6 to 17.8, and 5.3 to 6.0, respectively. Similarly, the elemental concentration of Sr and Ca varied from 224 to 229 ppm and 7.3 to 7.7%, respectively. The ratios of Zr/Al varied from 16.5 to 24.2. The values of weathering intensity CIA varied from 79 to 81 (**Supplementary Table 1**).

Zone 7

Zone 7 suggests the concentration of Al_2O_3, Fe_2O_3, and TiO_2 varied between 14.5–16.8%, 4.5–7.0%, and 0.79–0.98%, respectively. The oxide ratios of K_2O/Al_2O_3, Na_2O/TiO_2, CaO/TiO_2, and Fe_2O_3/TiO_2 varied from 0.18 to 0.20, 0.9 to 1.4, 5.6 to 12.2, and 5.6 to 7.9, respectively. Similarly, the elemental concentration of Sr and Ca varied from 161 to 216 ppm and

3.7 to 6.9%, respectively. The ratios of Zr/Al varied from 11.5 to 24.8. The values of weathering intensity CIA varied from 83 to 89 (**Supplementary Table 1**).

Mineral Magnetic Variations
Zone 1

Zone 1 shows the magnetic susceptibility (χ_{LF}) values varied between 1.18×10^{-8} m^3/kg and 1.97×10^{-8} m^3/kg, while the values of SIRM and χ_{arm} varied between 1.23–1.84 and 1.45×10^{-5}–5.88×10^{-5}, respectively. The increasing concentrations of χ_{LF}. SIRM, and χ_{arm} are indicative of the ferrimagnetic mineral signals. However, decreasing concentration of these parameters implies dominance of the anti-ferrimagnetic minerals within the section. Values of the S-ratio varied from 0.62 to 0.74, indicating the presence of low coercivity minerals (**Supplementary Table 2**).

Zone 2

Zone 2 shows the magnetic susceptibility (χ_{LF}) values varied between 1.55×10^{-8} m^3/kg and 1.56×10^{-8} m^3/kg, while the values of SIRM and χ_{arm} varied between 1.51–1.67 and 2.61×10^{-5}–3.60×10^{-5}, respectively. Values of the S-ratio varied from 0.63 to 0.66 (**Supplementary Table 2**).

Zone 3

Zone 3 suggests the magnetic susceptibility (χ_{LF}) values varied between 1.46×10^{-8} m^3/kg and 1.87×10^{-8} m^3/kg, while the values of SIRM and χ_{arm} varied between 1.39–2.16 and 2.82×10^{-5}–10×10^{-5}, respectively. Values of the S-ratio varied from 0.60 to 0.74 (**Supplementary Table 2**).

Zone 4

Zone 4 suggests the magnetic susceptibility (χ_{LF}) values varied between 1.82×10^{-8} m^3/kg and 1.88×10^{-8} m^3/kg, while the values of SIRM and χ_{arm} varied between 2.17–2.19 and 8.5×10^{-5}–8.9×10^{-5}, respectively. Values of the S-ratio varied from 0.76 to 0.77 (**Supplementary Table 2**).

Zone 5

Zone 5 suggests the magnetic susceptibility (χ_{LF}) values varied between 1.66×10^{-8} m^3/kg and 1.86×10^{-8} m^3/kg, while the values of SIRM and χ_{arm} varied between 1.98–2.19 and 7.10×10^{-5}–8.50×10^{-5}, respectively. Values of the S-ratio varied from 0.73 to 0.74 (**Supplementary Table 2**).

Zone 6

Zone 6 suggests the magnetic susceptibility (χ_{LF}) values varied between 1.56×10^{-8} m3/kg and 1.58×10^{-8} m3/kg, while the values of SIRM and χ_{arm} varied between 1.76–1.79 and 5.71×10^{-5}–6.12×10^{-5}, respectively. Values of the S-ratio varied from 0.75 to 0.77 (**Supplementary Table 2**).

Zone 7

Zone 7 suggests the magnetic susceptibility (χ_{LF}) values varied between 1.68×10^{-8} m^3/kg and 2.37×10^{-8} m^3/kg, while the values of SIRM and χ_{arm} varied between 1.91–2.76 and 6.82×10^{-5}–12.8×10^{-5}, respectively. Values of the S-ratio varied from 0.76 to 0.78 (**Supplementary Table 2**).

DISCUSSION

Approach: Role of Geochemistry and Magnetic Minerals in Paleoclimatic Reconstructions

The concentration of various oxides and elements is often derivative of weathering processes acting in the catchment of the basins. Major elemental concentration in sediments, mineral magnetics, and grain size often reflects the source of the origin, which were being used as effective proxies to demonstrate the intensity of chemical weathering, climate changes, and precipitation variations in the region (Staubwasser and Sirocko 2002; Yancheva et al., 2007; Tyagi et al., 2012; Clift et al., 2014; Das et al., 2017; Pillai et al., 2018; Ruifeng et al., 2020). The ratios like Na_2O/TiO_2, CaO/TiO_2, and Fe_2O_3/TiO_2 can be used to infer the changes in the paleoenvironmental condition (Pillai et al., 2018; Makwana et al., 2019). Increased values of Fe_2O_3/TiO_2 with lower values of Na_2O/TiO_2 and CaO/TiO_2 suggest increased precipitation, owing to the depletion of mobile elements like Ca and Na during erosion triggered by enhanced monsoon (Muhs et al., 2001; Kotlia and Joshi, 2013; Minyuk et al., 2013; Pillai et al., 2018). Hence, we assess the higher values of oxides like Al_2O_3, Fe_2O_3, and TiO_2 along with K_2O/Al_2O_3 and CIA (Chemical Index of Alteration) to mimic the enhanced monsoonal strength (Buggle et al., 2011; Pillai et al., 2018; Makwana et al., 2019). Similarly, concentration of magnetic minerals and their mineralogy have widely been used as surrogate to study the strength of the ISM (Basavaiah and Khadkikar, 2004; Warriar and Shankar, 2009). Magnetic susceptibility (χ) is controlled by the concentration and the grain-size distribution of ferromagnetic minerals and is strongly sensitive to variations of the local climate and constitutes an accurate proxy record, along with other parameters (Thompson and Oldfield, 1986; Phartiyal et al., 2003). The cumulative response of major oxide, elemental, CIA, and mineral magnetic properties is often touted to be a robust indicator of weathering intensity and is considered as a surrogate for reconstructing monsoonal strength (Warriar and Shankar, 2009; Prasad et al., 2007; 2014; Makwana et al., 2019).

Climatic Variability in Banni Plains Since the Mid-Holocene

Kachchh region in the western India experiences an arid climate and has attracted tremendous attention for its tectonic attributes (Chamyal et al., 2003). However, the landscape and its modulation with climatic forcings during the Holocene have been least explored (Pillai et al., 2017, 2018; Basu et al., 2019; Makwana et al., 2019; Sengupta et al., 2019). Our results reveal several alternate phases of wet and dry paleoclimatic conditions during the last five millennia from the Banni Plains (**Figure 3**).

Prior to 4,800 cal yr BP (Phase I)

The zone is marked by higher CIA values and other major elemental proxies, suggesting a higher chemical weathering under the relatively humid climatic regime (**Figure 4**). This is

further indicated by the higher concentration of detrital components such as Al_2O_3, TiO_2, and Fe_2O_3 vs. reduction of Na_2O/TiO_2, CaO/TiO_2, Zr/Al, CaO, and Sr (Peterson et al., 2000; Luckge et al., 2001; Kotlia and Joshi 2013; Pillai et al., 2018). Thus, collectively, the geochemical proxies indicate a strengthened monsoonal condition and intense chemical weathering at period prior to 4,800 years BP in the Banni Plains region. The mineral magnetic proxies which provide information about the type and concentration of magnetic grains transported in the catchment (Oldfield et al., 1994) also support the inferences drawn from the geochemical data. The lower values of χ_{lf} in phase one signify strengthened monsoonal condition, which leads to higher erosion and weathering that lowered the concentration of magnetic minerals. The values of the S-ratio also suggest a combined anti-ferro to ferrimagnetic mineral assemblage with dominance of ferrimagnetic minerals in phase I. The complied results of multi-proxies recommend the deposition of sediments that occurred under the relatively humid climatic condition in phase I (i.e., period prior to 4,800 years BP).

Thakur et al. (2019) based on palynological study form Harshad, western Saurashtra, reported a higher ISM precipitation during the 5,400 to 5,100 years BP period. Similar observations were also made by Kathayat et al. (2017) from the composite Sahiya $d^{18}O$ record from the Himalayas. Higher CIA and enhanced precipitation at 5.1 ka during the mature Harappan phase have also been reported by Ngangom et al (2016) from the nearby Eastern Great Rann of Kachchh. A similar, wet phase of ISM was recorded by Parsons Valley Lake, Tamilnadu, southern India (Raja et al., 2019).

### 4,400–4,800 cal yr BP Period (Phase II)

The zone is marked by abrupt changes to lower CIA values and other major elemental proxies, suggesting a weaker chemical weathering under arid climatic conditions (**Figure 4**). This abrupt aridity around 4,400 years BP has been one of the most discussed, although debated, causative factor for the deurbanization and decentralization of Harappans as a community that was primarily thriving on river-based resources (Staubwasser et al., 2003; Madella and Fuller, 2006; Dixit et al., 2014, 2018; Sengupta et al., 2019). Several studies have shown that the brief phase of aridity experienced in western India as well as the Himalayas led to the drying of water resources and speculated that this might have led the Harappan migrations to explore alternate water resources and settlement to smaller centers (Madella and Fuller, 2006). Based on our proxy data, which shows excessive deficient moisture conditions during this period (4,400–4,800 years BP), we support the earlier view that the prevalence of drought-like conditions affected the deurbanization of the Harappan settlement from the Western India.

Period Between 4,400 cal yr BP and 3,300 cal yr BP (Phase III)

Phase III is marked by fluctuating but an overall increasing value of mineral magnetic parameters, higher concentration of major, and lower ratios of geochemical proxies. An increase in CIA
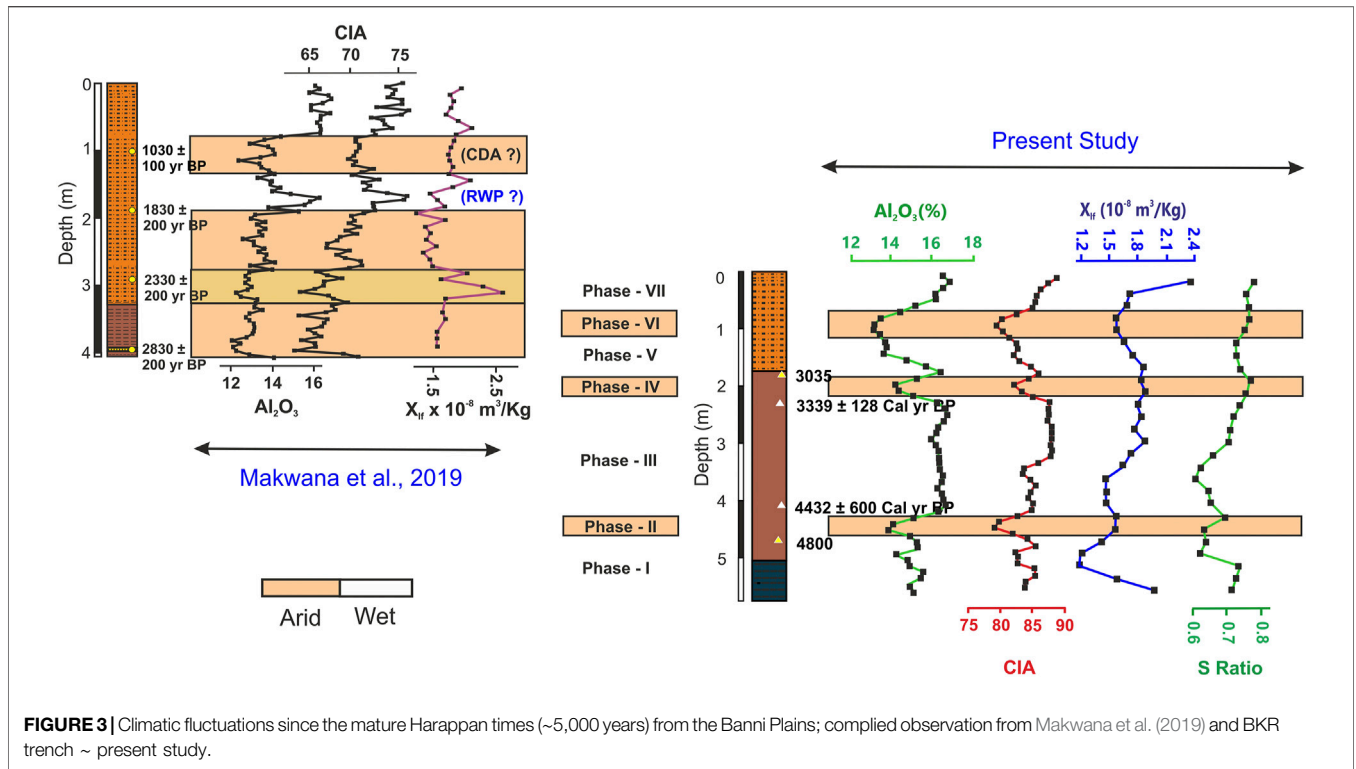
FIGURE 3 | Climatic fluctuations since the mature Harappan times (~5,000 years) from the Banni Plains; compiled observation from Makwana et al. (2019) and BKR trench ~ present study.
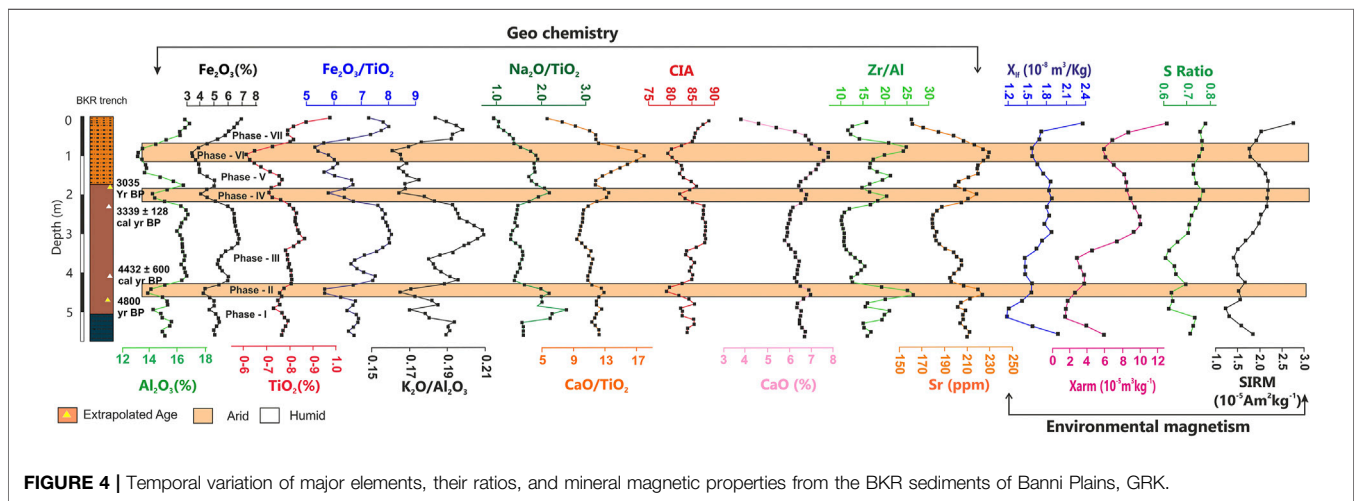
FIGURE 4 | Temporal variation of major elements, their ratios, and mineral magnetic properties from the BKR sediments of Banni Plains, GRK.

(>83%) hints an enhancement of chemical weathering signifying higher precipitation, which is also reflected in increasing concentration of major oxides such as Al_2O_3, Fe_2O_3, and TiO_2 (Anderson et al., 2004). A significant increasing trend is also noticeable in the ratios of K_2O/Al_2O_3 and Fe_2O_3/TiO_2 with lower concentration of Na_2O/TiO_2 and CaO/TiO_2 (**Figure 4**). Mineral magnetic parameters, that is, χ_{lf} and S-ratio, showed progressive decrease and thereafter increase in phase III, which indicates fluctuating but overall gradual increased precipitation/monsoon (**Figure 4**). Similar results of enhanced monsoonal strength have

also been reported by Pillai et al. (2017, 2018) from the Banni Plains during 4,600 and 2,500 years BP. This period was the initiation of deurbanization of the mighty Harappan civilization, which was marked by the migration of Harrapans from the well-established centers to other sites, owing to water source scarcity (Ponton et al., 2012; Dixit et al., 2014, 2018; Pokharia et al., 2017). On the contrary to this, recently, some studies have demonstrated change in farming pattern and other means for survival of the ancient settlers despite the aridity (Sarkar et al., 2020; Pokharia et al., 2017; Singh et al., 2018).

Period Between 3,300 cal yr BP and 3,000 cal yr BP (Phase IV)

The period from 3,300 years BP to 3,000 years BP experienced a relatively drier climate with reduced CIA values and abruptly decreasing concentration of major oxides such as Al_2O_3, Fe_2O_3, and TiO_2. The relative content of CaO, Sr, and Na_2O/TiO_2 increases as these mobile elements remain at the site due to the lack of hydrolysis. Prasad et al. (2014a) from the Wadhwana Lake in alluvial plains of Gujarat reported a short phase of low precipitation during 3,238–2,709 cal yr BP. Similar arid conditions are also reported from Rann sediments in northwest of the present site by Ngangom et al. (2016).

Contrastingly, Pillai et al. (2017, 2018) reported the period from 4,600 to 2,500 years BP as the period of enhanced monsoonal strength, owing to the coexistence of C4 and C3 vegetation along with geochemical composition of sediments due to chemical weathering. Recent studies from the Bednikund Lake, Himalayas, based on mineral magnetics, organic geochemistry, and grain size assemblages, also suggested an enhanced monsoonal strength during 3,380 and 2,830 cal yr BP. (Rawat et al., 2021).

Period During the Last 3,000 years (Phases V, VI, and VII in BKR Trench and BB Trench)

Makwana et al., 2019

The depiction of last three millennia has been done based on phases V, VI, and VII of BKR trench and previously reported BB trench from the northwest of the Banni Plains (Makwana et al., 2019). As we do not have age control on the top section of BKR, we only report that the phases V and VII show signs of strengthened monsoonal condition with enhanced values of CIA and associated geochemical proxies, whereas on the contrary, phase VI shows a relatively dip in CIA values and other oxides, hinting at a weaker chemical weathering, that is, arid climatic conditions.

On the contrary, the period from 2,900 years to 1900 years from BB trench site also supports an overall fluctuating to arid climatic condition with peak of that aridity around 2,400 years BP (Makwana et al., 2019). Pillai et al. (2018) from Luna core reported arid climatic condition during 3,000 to 2,500 years BP. Similarly, Quamar et al. (2021) studied a lacustrine sequence from central India and based on the pollen study reported a decline in strength of ISM during 3,000 to 2,600 years BP period. Similarly studies from the mudflats of Diu, Gujarat, are suggestive of the arid conditions during 2,640–1930 cal yr BP (Banerjee et al., 2017). This is in agreement with a long drought in the Thar Desert, India, between 3,600 and 2000 years BP (Bryson and Bryson, 1996; Enzel et al., 1999).

The period from 1900 years BP to 200 years BP shows three phases of prominent arid/humid climatic conditions (Makwana et al., 2019). These periods of arid/humid conditions coincide their timing with globally known events like the medieval climatic anomaly (MCA). These events have also been reported from regional archives in the past (Gupta et al., 2003; Sinha et al., 2007; Ngangom et al., 2012; Rajamanickam et al., 2017; Rawat et al., 2021). All the fluctuations from arid to humid climatic conditions during the last three millennia are abrupt in nature with sharp changes in proxy data (**Figure 3**). Previously, Makwana et al. (2019) reported a sedimentation rate of 1–2.2 mm/yr from the BB trench in the northwestern Banni Plains. The present BKR trench based on two AMS ^{14}C ages yields a sedimentation rate of 1.6 mm/yr during 4,432 to 3,339 cal yr BP period. The high sedimentation rate from BB and BKR trenches (>1 mm/yr) also aides this endeavor. Despite the poor chronological control, the presence of abrupt arid and humid periods during last two millennia is suggestive of Banni Plains being capable of being used as potential archive for studying climatic reconstructions.

CONCLUSION

Based on the multi-proxy dataset from the Banni Plains of the Kachchh region spanning last 5,000 years, the salient findings are as follows:

1. The periods from 4,800 to 4,400 cal yr BP are marked by abrupt drier climatic conditions in a multi-proxy dataset, which has also been reported by several other studies from the regional archives owing to the initiation of synchronous deurbanization of Harappan settlements. This is followed by a period from 3,300 to 3,000 cal yr BP and around 2,400 cal yr BP with pronounced aridity in the Banni Plain region.

2. The relatively humid climatic conditions were observed during >4,800 cal yr BP, 4,400 to 3,300 cal yr BP, 1900 to 1,400 years BP, and 900–550 years BP in the multi-proxy record. The late Harappan phase envisaged in the present study shows an intriguing gradual strengthening of the monsoonal intensity.

3. Based on preliminary results, the Banni Plains as an archive shows a high sedimentation rate, that is, > 1 mm/yr, which suggests it can act as a robust archive which can be tapped to be an excellent sedimentary record to reconstruct multi-decadal to centennial climatic events spanning the Holocene epoch.

Future studies from Banni Plains with relatively deeper information could likely aide in reconstructing the dynamics of the region spanning the entire Holocene epoch, as the present study validates the archiving potential of Banni sediments for reconstructing short and long spells of paleomonsoonal conditions.

DATA AVAILABILITY STATEMENT

The original contributions presented in the study are included in the article/**Supplementary Material**; further inquiries can be directed to the corresponding author.

AUTHOR CONTRIBUTIONS

The paper was written by NM and AD. The idea was conceptualized by NM, AD and SPP. The magnetic rsults and data was worked upon by BP. CV and AS contributed in field investigation and laboratory analysis. SPP supervised the work and edited the paper.

ACKNOWLEDGMENTS

SUPPLEMENTARY MATERIAL

The Supplementary Material for this article can be found online at: https://www.frontiersin.org/articles/10.3389/feart.2021.679689/full#supplementary-material

REFERENCES

Agnihotri, R., Bhattacharya, S. K., Sarin, M. M., and Somayajulu, B. L. K. (2003). Changes in Surface Productivity and Subsurface Denitrification during the Holocene: a Multiproxy Study from the Eastern Arabian Sea. *The Holocene* 13 (5), 701–713. doi:10.1191/2F0959683603hl656rp

Anderson, D. M., Baulcomb, C. K., Duvivier, A. K., and Gupta, A. K. (2010). Indian Summer Monsoon during the Last Two Millennia. *J. Quat. Sci.* 25 (6), 911–917. doi:10.1002/jqs.1369

Anderson, P. O. D., Worden, R. H., Hodgson, D. M., and Flint, S. (2004). Provenance Evolution and Chemostratigraphy of a Palaeozoic Submarine Fan-Complex: Tanqua Karoo Basin, South Africa. *Mar. Pet. Geology* 21, 555–577. doi:10.1016/j.marpetgeo.2004.01.004

Banerji, U., Bhusan, R., and Jull, A. J. T. (2017). Mid-late Holocene Monsoonal Records from the Partially Active Mudflats of Diu Island, Southern Saurashtra, Gujarat, Western India. *Quat. Int.* 443, 200–201. doi:10.1016/j.quaint.2016.09.060

Basavaiah, N. (2011). *Geomagnetism: Solid Earth and Upper Atmosphere Perspectives*. Dordrecht, Netherlands: Springer, 410.

Basavaiah, N., and Khadkikar, A. S. (2004). Environmental Magnetism and its Application towards Palaeomonsoon Reconstruction. *J. Indian Geophys. Union* 8 (1), 1–14.

Basu, S., Prasanta, S., Pillai, A. S., and Ambili, A. (2019). Response of Grassland Ecosystem to Monsoonal Precipitation Variability during the Mid-late Holocene: Inferences Based on Molecular Isotopic Records from Banni Grassland, Western India. *PLOS ONE* 14 (4), 0212743. doi:10.1371/journal.pone.0212743

Berkelhammer, M., Sinha, A., Mudelsee, M., Cheng, H., Edwards, L. R., and Cannariato, K. (2010). Persistent Multidecadal Power of the Indian Summer Monsoon. *Earth Planet. Sci. Lett.* 290, 166–172. doi:10.1016/j.epsl.2009.12.017

Bianchi, G. G., and Mc Cave, I. N. (1999). Holocene Periodicity in North Atlantic Climate and Deep Ocean Flow South of Iceland. *Nature* 397, 515–517. Available at: https://www.nature.com/articles/17362.

Biswas, S. K. (1987). Regional Tectonic Framework, Structure and Evolution of the Western Marginal Basins of India. *Tectonophysics* 135, 307–327. doi:10.1016/0040-1951(87)90115-6

Brooks, N. (2006). Cultural Responses to Aridity in the Middle Holocene and Increased Social Complexity. *Quat. Int.* 151 (1), 29–49. doi:10.1016/j.quaint.2006.01.013

Bryson, R. U., and Bryson, R. A. (1996). Application of a Global Volcanicity Time-Series on High-Resolution Paleoclimatic Modeling of the Eastern Mediterranean. *Water Sci. Technol. Libr.* 31, 1–19. doi:10.1007/978-94-017-3659-6_1

Buggle, B., Glaser, B., Hambach, U., Gerasimenko, N., and Markovic, S. (2011). An Evaluation of Geochemical Weathering Indices in Loess–Paleosol Studies. *Quat. Int.* 240, 12–21. doi:10.1016/j.quaint.2010.07.019

Burnes, A. (1834). Memoir on the Eastern Branch of the River Indus, Giving an Account of the Alterations Produced on it by an Earthquake, Also a Theory of the Formation of the Runn, and Some Conjectures on the Route of Alexander the Great; Drawn up in the Years 1827-1828. *Trans. R. Asiatic Soc. Great Britain Ireland* 3, 550–588.

Chamyal, L. S., Maurya, D. M., and Rachna, R. (2003). Fluvial Systems of the Dry Lands of Western India: a Synthesis of Late Quaternary Environmental and Tectonic Changes. *Quat. Int.* 104, 69–86. doi:10.1016/s1040-6182(02)00136-2

Chauhan, O. S., Vogelsang, E., Basavaiah, N., and Syed, A. K. (2009). Reconstruction of the Variability of the Southwest Monsoon during the Past 3 Ka, from the continental Margin of the southeastern Arabian Sea. *J. Quat. Sci.* 25, 798–807. doi:10.1002/jqs.1359

Clift, P. D., Wan, S., and Blusztajn, B. (2014). Reconstructing Chemical Weathering, Physical Erosion and Monsoon Intensity since 25 Ma in the Northern South China Sea: A Review of Competing Proxies. *Earth Sci. Rev.* 130, 86–102. doi:10.1016/j.earscirev.2014.01.002

Das, A., Prizomwala, S., Makwana, N., and Thakkar, M. (2017). Late Pleistocene-Holocene Climate and Sea Level Changes Inferred Based on the Tidal Terrace Sequence, Kachchh, Western India. *Palaeogeogr. Palaeoclimatol. Palaeoecol.* 473, 82–93. doi:10.1016/j.palaeo.2017.02.026

Dixit, Y., Hodell, D. A., Giesche, A., Tandon, S. K., Gázquez, F., Saini, H. S., et al. (2018). Intensified Summer Monsoon and the Urbanization of Indus Civilization in Northwest India. *Nat. Scientific Rep.* 8, 4225. doi:10.1038/s41598-018-22504-5

Dixit, Y., Hodell, D. A., Sinha, R., and Petrie, C. A. (2014). Abrupt Weakening of the Indian Summer Monsoon at 8.2 Kyr B.P. *Earth Planet. Sci. Lett.* 391, 16–23. doi:10.1130/G35236.1

Dutta, K., Bhushan, R., and Somayajulu, B. L. K. (2001). ΔR Correction Values for the Northern Indian Ocean. *Radiocarbon*. 43, Nr 2A, 483–488. doi:10.1017/s0033822200038376

Enzel, Y., Ely, L. L., Mishra, S., Ramesh, R., Amit, R., Lazar, B., et al. (1999). High Resolution Holocene Environmental Changes in the Thar Desert, Northwestern India. *Science* 284, 125–127. doi:10.1126/science.284.5411.125

Galili, E., Weinstein-Evron, M., and Ronen, A. (1988). Holocene Sea-Level Changes Based on Submerged Archaeological Sites off the Northern Carmel Coast in Israel. *Quat. Res.* 29, 36–42. doi:10.1016/0033-5894(88)90069-5

Gaur, A. S., Vora, K. H., Sundaresh, R., Murali, R. M., and Jaya kumar, S. (2013). Was the Rann of Kachchh Navigable during the Harappan Times (Middle Holocene)? an Archaeological Perspective. *Curr. Sci.* 105, 1485–1491.

Giosan, L., Clift, P. D., Macklin, M. G., Fuller, D. Q., Constantinescu, S., Durcan, J. A., et al. (2012). Fluvial Landscape of the Harappan Civilization. *Proc. Natl. Acad. Sci.* 109 (26), 1688–1694. doi:10.1073/pnas.1112743109

Glennie, K. W., and Evans, G. (1976). A Reconnaissance of the Recent Sediments of the Ranns of Kutch, India. *Sedimentology* 23, 625–647. doi:10.1111/j.1365-3091.1976.tb00098.x

Gupta, A., Anderson, D., and Overpeck, J. (2003). Abrupt Changes in the Asian Southwest Monsoon during the Holocene and Their Links to the North Atlantic Ocean. *Lett. Nat.* 421 (6921), 354–357. doi:10.1038/nature01340

Gupta, S. K. (1975). Silting of the Rann of the Kutch during the Holocene. *Indian J. Earth Sci.* 2, 163–175.

Khatayat, G., Cheng, H., Sinha, A., Yi, L., Xianglei, Li., Zhang, H., et al. (2017). The Indian Monsoon Variability and Civilization Changes in the Indian Subcontinent. *Sci. Adv.* 3 (12). doi:10.1126/sciadv.1701296

Khonde, N., Maurya, D. M., and Chamyal, L. S. (2017a). Late Pleistocene-Holocene clay mineral Record from the Great Rann of Kachchh basin, Western India: Implications for Palaeoenvironments and Sediment Sources. *Quat. Int.* 443, 86–98. doi:10.1016/j.quaint.2016.07.024

Khonde, N., Singh, S., Maurya, D. M., Rai, V. K., Chamyal, L. S., and Giosan, L. (2017b). Tracing the Vedic Saraswati River in the Great Rann of Kachchh. *Scientific Rep.* 7 (1). doi:10.1038/s41598-017-05745-8

Kotlia, B, S., and Joshi, L. M. (2013). Late Holocene Climatic Changes in Garhwal Himalaya. *Curr. Sci.* 104, 7.

Lamb, H. H. (1985). *Climatic History and the Future*. Princeton University Press.

Laskar, A. H., Yadava, M. G., Sharma, N., and Ramesh, R. (2013a). Late-Holocene Climate in the Lower Narmada valley, Gujarat, Western India, Inferred Using Sedimentary Carbon and Oxygen Isotope Ratios. *The Holocene* 23 (8), 1115–1122. doi:10.1177/2F0959683613483621

Lückge, A., Doose-Rolinski, H., Khan, A. A., Schulz, H., and Von Rad, U. (2001). Monsoonal Variability in the Northeastern Arabian Sea during the Past 5000 years: Geochemical Evidence from Laminated Sediments. *Palaeogeogr. Palaeoclimatol. Palaeoecol.* 167 (3-4), 273–286. doi:10.1016/S0031-0182(00)00241-8

Madella, M., and Fuller, D. Q. (2006). Palaeoecology and the Harappan Civilisation of South Asia: Reconsideration. *Quat. Sci. Rev.* 25 (11-12), 1283–1301. doi:10.1016/j.quascirev.2005.10.012

Makwana, N. M., Prizomwala, S. P., Chauhan, G., Phartiyal, B., and Thakkar, M. G. (2019). Late Holocene Palaeo-Environmental Change in the Banni Plains, Kachchh, Western India. *Quat. Int.* 507, 197–205. doi:10.1016/j.quaint.2018.11.028

Maurya, D., Khonde, N., Das, A., Chowksey, V., and Chamyal, L. (2013). Subsurface Sediment Characteristics of the Great Rann of Kachchh, Western India Based on Preliminary Evaluation of Textural Analysis of Two Continuous Sediment Cores. *Curr. Sci.* 104 (8), 1071–1077. Available at:

Minyuk, P. S., Borkhodoev, V. Ya., and Wennrich, V. (2013). Inorganic Data from El'gygytgyn Lake Sediments: Stages 6-11. *Clim. past Discuss.* 9, 393–433. doi:10.5194/cpd-9-393-2013

Muhs, D. R., Bettis, E. A., Been, J., and Mc Geehin, J. P. (2001). Impact of Climate and Parent Material on Chemical Weathering in Loess Derived Soils of the Mississippi River Valley. *Soil Sci. Soc. America J.* 65, 1761–1777. doi:10.2136/sssaj2001.1761

Nesbitt, H. W., and Young, G. M. (1982). Early Proterozoic Climates and Plate Motions Inferred from Major Element Chemistry of Lutites. *Nature* 299, 5885715–5885717. doi:10.1038/299715a0

Ngangom, M., Bhandari, S., Thakkar, M. G., Shukla, A. D., and Juyal, N. (2016). Mid-Holocene Extreme Hydrological Events in the Eastern Great Rann of Kachchh, Western India. *Quat. Int.* 443, 188–199. doi:10.1016/j.quaint.2016.10.017

Ngangom, M., Thakkar, M., Bhushan, R., and Juyal, N. (2012). Continental–marine Interaction in the Vicinity of the Nara River during the Last 1400 years, Great Rann of Kachchh, Western India. *Curr. Sci.* 103 (11), 1339–1342. Available at: https://www.jstor.org/stable/24089154.

Oldfield, F. (1994). Toward the Discrimination of fine-grained Ferrimagnets by Magnetic Measurements in lake and Near-shore marine Sediments. *J. Geophys. Res. Solid Earth* 99 (B5), 9045–9050. doi:10.1029/93JB03137

Petterson, L. C., Haug, G. H., Hughen, K. A., and Rohl, U. (2000). Rapid Changes in the Hydrologic Cycle of the Tropical Atlantic during the Last Glacial. *Science* 290, 1947–1951. doi:10.1126/science.290.5498.1947

Phartiyal, B., Appel, E., Blaha, U., Hoffmann, V., and Kotlia, B. S. (2003). Palaeoclimatic Significance of Magnetic Properties from Late Quaternary Lacustrine Sediments at Pithoragarh, Kumaun Lesser Himalaya, India. *Quat. Int.* 108, 51–62. doi:10.1016/S1040-6182(02)00193-3

Pillai, A. S., Ambili, A., Prasad, V., Manoj, M. C., Varghese, S., Prasanta, S., et al. (2018). Multi-proxy Evidence for an Arid Shift in the Climate and Vegetation of the Banni Grasslands of Western India during the Mid to Late Holocene. *The Holocene* 28 (7), 1057–1070. doi:10.1177/0959683618761540

Pillai, A. S., Ambili, A., Sankaran, M., Prasanta, S., Jha, D., and Ratnam, J. (2017). Mid-late Holocene Vegetation Response to Climatic Drivers and Biotic Disturbances in the Banni Grasslands of Western India. *Palaeogeogr. Palaeoclimatol. Palaeoecol.* 485, 869–878. doi:10.1016/j.palaeo.2017.07.036

Possehl, G. (2002). *The Indus Civilization: A Contemporary Perspective*. Lanham, MD: Altamira Press.

Prasad, S., Anoop, A., Riedel, N., Sarkar, S., Menzel, P., Basavaiah, N., et al. (2014b). Prolonged Monsoon Droughts and Links to Indo-Pacific Warm Pool: A Holocene Record Rom Lonar Lake, central India. *Earth Planet. Sci. Lett.* 391, 171–182. doi:10.1016/j.epsl.2014.01.043

Prasad, V., Farooqui, A., Sharma, A., Phartiyal, B., Chakraborty, S., Raj, R., et al. (2014a). Mid-late Holocene Monsoonal Variations from mainland Gujarat, India: a Multi-Proxy Study for Evaluating Climate Culture Relationship. *Palaeogeogr. Palaeoclimatol. Palaeoecol.* 397, 38–51. doi:10.1016/j.palaeo.2013.05.025

Prasad, V., Phartiyal, B., and Sharma, A. (2007). Evidence of Enhanced winter Precipitation and the Prevalence of a Cool and Dry Climate during the Mid to Late Holocene in mainland Gujarat, India. *The Holocene* 17 (7), 889–896. doi:10.1177/0959683607082403

Quamar, M. F., and Chauhan, M. S. (2014). Signals of Medieval Warm Period and Little Ice Age Southwestern Madhya Pradesh (India): A Pollen-Inferred Late-Holocene Vegetation and Climatic Change. *Quat. Int.* 325, 74–82. doi:10.1016/j.quaint.2013.07.011

Quamar, M. F., Kar, R., and Thakur, B. (2021). Vegetation Response to the Indian Summer Monsoon (ISM) Variability during the Late-Holocene from the central Indian Core Monsoon Zone. *The Holocene* 31 (7), 1197–1211. doi:10.1177/09596836211003191

Raja, P., Achyuthan, H., Farooqui, A., Ramesh, R., Kumar, P., and Chopra, S. (2019). Tropical Rainforest Dynamics and Palaeoclimate Implications since the Late Pleistocene, Nilgiris, India. *Quat. Res.* 91 (1), 367–382. doi:10.1017/qua.2018.58

Rajmanickam, V., Achyuthan, H., Eastoe, C., and Farooqui, A. (2017). Early-Holocene to present palaeoenvironmental shifts and short climate events from the tropical wetland and lake sediments, Kukkal Lake, Southern India: Geochemistry and palynology. *The Holocene* 27 (3), 404–417. doi:10.1177/0959683616660162

Rawat, V., Rawat, S., Srivastava, P., Negi, P. S., Prakasam, M., and Kotlia, B. S. (2021). Middle Holocene Indian Summer Monsoon Variability and its Impact on Cultural Changes in the Indian Subcontinent. *Quat. Sci. Rev.* 255, 106825. doi:10.1016/j.quascirev.2021.106825

Roy, B., and Merh, S. (1981). The Great Rann of Kutch: Intriguing Quaternary Terrain. *Recent Researches Geology.* 9, 100.

Ruifeng, M., Wei1, Z., and Chanyu, Y. (2020). Multi-proxy Records of Holocene Fluvio-Lacustrine Sediments in the Southern Liaodong Peninsula, China. *E3S Web of Conferences* 165, 03023. doi:10.1051/e3sconf/202016503023

Sanwal, J., Kotlia, B., Rajendran, C., Ahmad, S., Rajendran, K., and Sandiford, M. (2013). Climatic Variability in Central Indian Himalaya during the Last ~ 1800 years: Evidence from a High Resolution Speleothem Record. *Quat. Int.* 304, 183–192. doi:10.1016/j.quaint.2013.03.029

Sarkar, A., Mukherjee, A. D., Sharma, S., Sengupta, T., Ram, F., Bera, M. K., et al. (2020). New Evidence of Early Iron Age to Medieval Settlements from the Southern Fringe of Thar Desert (Western Great Rann of Kachchh), India: Implications to Climate-Culture Co-evolution. *Archaeological Res. Asia* 21, 2352–2267. doi:10.1016/j.ara.2019.100163

Sengupta, T., Mukherjee, A. D., Bhusan, R., Ram, F., Bera, M. K., Raj, H., et al. (2019). Did the Harappan Settlement of Dholavira (India) Collapse during the Onset of Meghalayan Stage Drought? *J. Quat. Sci.* 35 (3), 382–395. doi:10.1002/jqs.3178

Sinha, A., Cannariato, K. G., Stott, L. D., Cheng, H., Edwards, R. L., Yadava, M. G., et al. (2007). A 900-year (600 to 1500 AD) Record of the Indian Summer Monsoon Precipitation from the Core Monsoon Zone of India. *Geophys. Res. Lett.* 34, 16707. doi:10.1029/2007GL030431

Sridhar, A., Chamyal, L. S., and Patel, M. (2014a). Palaeoflood Record of High-Magnitude Events during Historical Time in the Sabarmati River, Gujarat. *Curr. Sci.* 107 (4), 675–679. Available at: https://www.jstor.org/stable/24103542

Staubwasser, M., Sirocko, F., Grootes, P. M., and Segl, M. (2003). Climate Change at the 4.2 Ka BP Termination of the Indus valley Civilization and Holocene South Asian Monsoon Variability. *Geophys. Res. Lett.* 30 (8), 14–25. doi:10.1029/2002GL016822

Stuiver, M., Reimer, P. J., and Reimer, R. W., (2018). CALIB 7.1 [WWW program] at http://calib.org, accessed. 8-13.

Thakur, B., Seth, P., Sharma, A., Pokharia, A. K., Spate, M., and Farooqui, S. (2019). Linking Past Cultural Developments to Palaeoenvironmental Changes from 5000 BP to Present: A Climate-Culture Reconstruction from Harshad Estuary, Saurashtra, Gujarat, India. *Quat. Int.* 507, 188–196. doi:10.1016/j.quaint.2019.01.019

Thompson, R., and Oldfield, F. (1986). *Environmental Magnetism*. London: Allen & Unwin, 227.

Tyagi, A. K., Shukla, A. D., Bhushan, R., Thakker, P. S., Thakkar, M. G., and Juyal, N. (2012). Mid-Holocene Sedimentation and Landscape Evolution in the Western Great Rann of Kachchh, India. *Geomorphology* 151-152, 89–98. doi:10.1016/j.geomorph.2012.01.018

Walden, J. (1999). "Remanence Measurements," in *Environmental Magnetism - A Practical Guide, Technical Guide No. 6*. Editors J. Walden, J. P. Smith, and F. Oldfield (London: Quaternary Research Association), 63–88.

Warrier, A., and Shankar, R. (2009). Geochemical Evidence for the Use of Magnetic Susceptibility as a Paleorainfall Proxy in the Tropics. *Chem. Geology* 265, 553–562. doi:10.1016/j.chemgeo.2009.05.023

Wright, R. P., Bryson, R., and Schuldenrein, J. (2008). Water Supply and History: Harappa and the Beas Regional Survey. *Antiquity* 8, 37–48. doi:10.1017/S0003598X00096423

Yancheva, G., Nowaczyk, N. R., Mingram, J., Dulski, P., Schettler, G., Negendank, F. W., et al. (2007). Influence of the Intertropical Convergence Zone on the East Asian Monsoon. *Nat. Lett.* 445 (7123), 74–77. doi:10.1038/nature05431